

Photoreduction of 1,2-Dichloroalkanes and 1,2-Dichloroalkenes by Tetrakis(diphenyl phosphato)dimolybdenum(II,II)

Tsui-Ling C. Hsu, I-Jy Chang, Donald L. Ward, and Daniel G. Nocera*

Department of Chemistry, Michigan State University, East Lansing, Michigan 48824

Received August 18, 1993*

The quadruply bonded metal–metal complex $\text{Mo}_2[\text{O}_2\text{P}(\text{OC}_6\text{H}_5)_2]_4$ reduces 1,2-dichloroalkanes and 1,2-dichloroalkenes upon its irradiation with visible light ($\lambda_{\text{exc}} \geq 495 \text{ nm}$). The inorganic product of the photochemistry in all cases is the $\text{Mo}^{\text{II}}\text{Mo}^{\text{III}}$ mixed-valence binuclear complex $\text{Mo}_2[\text{O}_2\text{P}(\text{OC}_6\text{H}_5)_2]_4^+$, which has been structurally characterized. Green prismatic crystals of the tetrafluoroborate salt are triclinic with a $P\bar{1}$ space group: $a = 10.917(8)$, $b = 11.793(4)$, $c = 12.430(4) \text{ \AA}$; $\alpha = 63.45(2)$, $\beta = 70.38(4)$, $\gamma = 70.64(5)^\circ$; $V = 1316.8(12) \text{ \AA}^3$; $Z = 1$. The structure was refined to values of $R = 0.036$ and $R_w = 0.043$. The Mo–Mo bond distance of 2.191 \AA is 0.05 \AA greater than its quadruple bond parent complex, $\text{Mo}_2[\text{O}_2\text{P}(\text{OC}_6\text{H}_5)_2]_4 \cdot 2\text{THF}$. The mixed-valence dimer shows a vibrationally-structured $\delta \rightarrow \delta^*$ (${}^2B_{1u} \leftarrow {}^2B_{2g}$) absorption band in the near-infrared spectral region ($\lambda_{\text{max}} = 1469 \text{ nm}$, $\epsilon = 142 \text{ M}^{-1} \text{ cm}^{-1}$) with a 308-cm^{-1} energy spacing, which is consistent with a progression in the symmetric metal–metal stretching vibration. The mixed-valence complex is reversibly reduced and oxidized by one-electron ($E_{1/2}(\text{Mo}_2(\text{II,III}/\text{II,II})) = +0.067 \text{ V}$ and $E_{1/2}(\text{Mo}_2(\text{III,III}/\text{II,III})) = +0.997 \text{ V}$ vs SCE). The nature of the organic product resulting from $\text{Mo}_2[\text{O}_2\text{P}(\text{OC}_6\text{H}_5)_2]_4$ photochemistry depends on the organic substrate. For 1,2-dichloroalkanes, photoreaction is facile and affords the olefin ($\phi_p(1,2\text{-dichloroethane}) = 0.029$; $\phi_p(1,2\text{-trans-dichlorocyclohexane}) = 0.040$), whereas photoreaction of 1,2-dichloroalkenes yields monohalogenated alkenes ($\phi_p(1,2\text{-cis-dichloroethylene}) = 5.5 \times 10^{-6}$; $\phi_p(o\text{-dichlorobenzene}) = 1.4 \times 10^{-4}$).

Introduction

Quadruply bonded metal–metal ($\text{M}^4\text{-M}$) complexes offer an unique opportunity to explore excited-state oxidation–reduction chemistry owing to the presence of low-energy excited states localized at a coordinatively unsaturated, redox-active bimetallic core. Nevertheless, until recently,¹ photoactivation of substrates by $\text{M}^4\text{-M}$ complexes often occurred from metal-localized states that are high in energy.^{2,3} For instance, when acidic aqueous solutions of $\text{Mo}^{\text{II}}\text{Mo}^{\text{II}}$ phosphate dimer $\text{Mo}_2(\text{HPO}_4)_4^{4-}$ are irradiated with ultraviolet light, the two-electron oxidized triple bonded $\text{Mo}^{\text{III}}\text{Mo}^{\text{III}}$ complex $\text{Mo}_2(\text{HPO}_4)_4^{2-}$ and hydrogen are produced.² This photochemistry is consistent with the general observation that the lowest energy ${}^1(\delta\delta^*)$ excited state of $\text{M}^4\text{-M}$ complexes in aqueous solution is photochemically inert. One reason for this photoinactivity is the propensity of the ${}^1(\delta\delta^*)$ excited state to be efficiently quenched by protons in aqueous solutions.^{1c} This suggested to us that the chemistry of the ${}^1(\delta\delta^*)$ excited state could be exploited by undertaking studies of $\text{Mo}^{\text{II}}\text{Mo}^{\text{II}}$ phosphates in aprotic environments, where the energy-wasting, proton-quenching reactions of the ${}^1(\delta\delta^*)$ excited state would be circumvented thus preserving it for reaction with substrate. In this manner, substrate activation processes of $\text{M}^4\text{-M}$ species might be achieved with visible light.

To this end, we undertook studies to prepare and characterize dimolybdenum dialkyl and diaryl phosphates $\text{Mo}_2[\text{O}_2\text{P}(\text{OR})_2]_4$ ($\text{R} = \text{phenyl, alkyl}$). We now report the synthesis and charac-

terization of the quadruply bonded $\text{Mo}^{\text{II}}\text{Mo}^{\text{II}}$ and mixed-valence $\text{Mo}^{\text{II}}\text{Mo}^{\text{III}}$ tetrakis(diphenyl phosphates) and their photochemistry with halocarbon substrates. A preliminary account⁴ of our studies on these systems has been communicated. During our work, a study of the $\text{Mo}^{\text{II}}\text{Mo}^{\text{II}}$ and $\text{Mo}^{\text{II}}\text{Mo}^{\text{III}}$ diphenyl phosphates was also reported by Morrow and Trogler (MT).⁵ In the case of the former, the compound was isolated and structurally characterized, whereas the latter has yet to be structurally identified. Inasmuch as the analytical and spectroscopic results of the $\text{Mo}^{\text{II}}\text{Mo}^{\text{II}}$ compound prepared by these authors are consistent with the compound reported herein, we primarily focus on the characterization of the $\text{Mo}^{\text{II}}\text{Mo}^{\text{III}}$ compound and only discuss new chemistry of the quadruple bond species.

Experimental Section

General Procedures. All chemicals were reagent grade and were used as received unless otherwise noted. Syntheses of the dimolybdenum tetrakis(diphenyl phosphates) were performed under argon by using standard Schlenk techniques. Methanol used for syntheses was refluxed over Na for no less than 6 h and freshly distilled prior to use. The amount of Na added to MeOH was 20% more than the amount required to react with the water contained in a freshly opened bottle. All solvents used for spectroscopic, electrochemical, and photochemical experiments were purchased from Burdick and Jackson Laboratories (Spectroscopic grade). Purified solvents were stored in glass containers that consisted of a 1-L flask equipped with a Kontes high-vacuum valve. 1,2-Dichloroethane, 1,2-dichloroethylene, and 1,2-dichlorocyclohexane were degassed by seven freeze–pump–thaw cycles and stored over activated (heated to 250°C under 10^{-6} Torr dynamic vacuum for 12 h) Linde 4- \AA molecular sieves contained in a storage flask; *ortho*-dichlorobenzene was refluxed over P_2O_5 under a nitrogen atmosphere. Tetrahydrofuran and benzene were subjected to seven freeze–pump–thaw cycles and subsequently distilled into flasks containing sodium–potassium alloy with a small amount of benzophenone; the purple ketyl form of benzophenone formed over a 2-day period.

Syntheses of Dimolybdenum Complexes. The $\text{Mo}^{\text{II}}\text{Mo}^{\text{II}}$ tetrakis(diphenyl phosphate) was prepared by a simple ligand substitution reaction.

* Abstract published in *Advance ACS Abstracts*, May 1, 1994.

- (1) (a) Partigianoni, C. M.; Turró, C.; Hsu, T.-L. C.; Chang, I.-J.; Nocera, D. G. In *Photosensitive Metal–Organic Systems*; Kutal, C., Serpone, N., Eds.; Advances in Chemistry Series 238; American Chemical Society: Washington, DC, 1993; p 147. (b) Partigianoni, C. M.; Turró, C.; Shin, Y.-g. K.; Motry, D. H.; Kadis, J.; Dulebohn, J. I.; Nocera, D. G. *Mixed Valency Systems: Applications in Chemistry, Physics, and Biology*; Prassides, K., Ed.; Kluwer Academic: Dordrecht, The Netherlands, 1991; p 91. (c) Partigianoni, C. M.; Chang, I.-J.; Nocera, D. G. *Coord. Chem. Rev.* **1990**, *97*, 105.
- (2) Chang, I.-J.; Nocera, D. G. *J. Am. Chem. Soc.* **1987**, *109*, 4901.
- (3) (a) Erwin, D. K.; Geoffroy, G. L.; Gray, H. B.; Hammond, G. S.; Solomon, E. I.; Trogler, W. C.; Zagars, A. A. *J. Am. Chem. Soc.* **1977**, *99*, 3620. (b) Trogler, W. C.; Erwin, D. K.; Geoffroy, G. L.; Gray, H. B. *J. Am. Chem. Soc.* **1978**, *100*, 1160.

(4) Chang, I.-J.; Nocera, D. G. *Inorg. Chem.* **1989**, *28*, 4309.

(5) Morrow, J. R.; Trogler, W. C. *Inorg. Chem.* **1989**, *28*, 615.

Table 1. Crystallographic Data for Mo₂[O₂P(OC₆H₅)₂]₄BF₄

chem formula	C ₄₈ H ₄₀ BF ₄ Mo ₂ O ₁₆ P ₄	<i>V</i>	1316.8(12) Å ³
fw	1275.43	<i>Z</i>	1
space group	P $\bar{1}$ (No. 2)	<i>T</i>	29(1) °C
<i>a</i>	10.917(8) Å	λ (Mo K α)	0.710 73 Å
<i>b</i>	11.793(4) Å	ρ_{calc}	1.61 g cm ⁻³
<i>c</i>	12.430(4) Å	μ	6.6 cm ⁻¹
α	63.45(2)°	<i>R</i> (<i>F</i> _o)	0.036 ^a
β	70.38(4)°	<i>R</i> _w (<i>F</i> _o)	0.043 ^b
γ	70.64(5)°		

^a $R = \sum ||F_o| - |F_c|| / \sum |F_o|$. ^b $R_w = [\sum w(|F_o| - |F_c|)^2 / \sum w|F_o|^2]^{1/2}$; $w = 1/(\sigma^2|F_o|)$.

Table 2. Selected Atomic Positional Parameters and Equivalent Isotropic Displacement Parameters (Å²) for Mo₂[O₂P(OC₆H₅)₂]₄BF₄

atom	<i>x</i>	<i>y</i>	<i>z</i>	<i>B</i> _{eq}
Mo(1)	0.00740(3)	-0.09325(3)	-0.00348(2)	3.252(6)
P(1)	0.25809(9)	0.01679(8)	-0.16562(8)	3.75(2)
P(2)	0.1358(1)	-0.13280(8)	0.19944(7)	3.80(2)
O(1)	0.1984(2)	-0.1007(2)	-0.1154(2)	3.97(6)
O(2)	-0.1790(2)	-0.1162(2)	0.1088(2)	4.14(6)
O(3)	0.0878(3)	-0.2039(2)	-0.1512(2)	4.14(6)
O(4)	-0.0728(3)	-0.0106(2)	-0.1584(2)	4.02(6)
O(5)	0.2890(3)	-0.1405(2)	0.1532(2)	4.29(6)
O(6)	0.4008(3)	-0.0181(2)	-0.1440(2)	4.49(6)
O(7)	0.2686(3)	0.0753(2)	-0.3087(2)	4.25(6)
O(8)	0.1044(3)	-0.2048(2)	0.3428(2)	4.76(6)

The anion (C₆H₅O)₂PO₂⁻ was generated by stirring 3.25 g of (C₆H₅O)₂P(O)OH (13 mmol) with 0.702 g of NaOMe (13 mmol) in 60 mL of MeOH. After 10 min, 0.5 g of (NH₄)₂Mo₂Cl₉·H₂O (0.807 mmol) was added to the above solution, which was then heated to reflux for 3 h. A pink precipitate, formed during refluxing, was collected by suction filtration and washed with three 15 mL portions of MeOH. Aliquots for all washings were delivered by cannula. The solid was dried and stored under vacuum. Yield: 76%. Suitable crystals of Mo₂[O₂P(OC₆H₅)₂]₄·2THF for X-ray structural determination were obtained by layering a tetrahydrofuran solution of Mo₂[O₂P(OC₆H₅)₂]₄ with cyclohexane in a Schlenk tube. Anal. Calcd (found) for Mo₂C₄₈H₄₀O₁₆P₄·2C₂H₆O: Mo, 14.4 (14.87); P, 9.29 (9.17); C, 50.46 (49.93); H, 4.24 (4.15). The Mo^{II}Mo^{III} tetrakis(diphenyl phosphate) complex is extremely air-sensitive, decomposing within seconds upon exposure to air. This binuclear complex is not soluble in most organic solvents, but it exhibits fairly good solubilities in halogenated hydrocarbons and THF.

The mixed-valent Mo^{II}Mo^{III} tetrakis(diphenyl phosphate) complex is prepared by direct oxidation of the Mo^{II}Mo^{II} complex. Rigorously stirred CH₂Cl₂ solutions of 1.001 g (0.85 mmol) of Mo₂[O₂P(OC₆H₅)₂]₄ turn from pink to a green hue within 45 min after the addition 0.099 g (0.85 mmol) of NOBF₄ (Aldrich Chemical). The volume of solution was reduced to 10 mL by vacuum distillation, whereupon 50 mL of cyclohexane was added. A greenish-silver precipitate formed immediately. The solid was collected by suction filtration. Anal. Calcd (found) for Mo₂C₄₈H₄₀O₁₆P₄BF₄: C, 45.20 (41.23); H, 3.16 (3.15); P, 9.71 (9.33); F, 5.96 (6.13). Yield: 85%. X-ray quality crystals were obtained by layering a dichloromethane solution of Mo₂[O₂P(OC₆H₅)₂]₄BF₄ with cyclohexane in a Schlenk tube. The Mo^{II}Mo^{III} tetrakis(diphenyl phosphate) complex is not as air-sensitive as the corresponding Mo^{II}Mo^{II} dimer. Solid exposed to air is stable but for no longer than 30 min. Yet solutions of Mo₂[O₂P(OC₆H₅)₂]₄BF₄ are extremely air-sensitive. Both the solid and solution are thermally unstable, decomposing when heated higher than 80 °C.

Structure Determination of Mo₂[O₂P(OC₆H₅)₂]₄BF₄. Crystal structure determinations were performed in the X-ray Crystal Structure Facility at Michigan State University. Preliminary examination and data collection were performed with Mo K α radiation ($\lambda = 0.710 73$ Å) on a Nicolet P3F diffractometer. The intensity data were collected at 29 °C by using θ - 2θ scans at a rate of 4°/min (in 2θ) to a maximum 2θ of 55°. The ratio of peak counting time to background counting time was 1:1. The diameter of the incident beam collimator was 1.5 mm and the crystal to detector distance was 19 cm. Table 1 lists crystal parameters and details of intensity collection and refinement, and the selected positional parameters are given in Table 2. Complete tables of positional parameters, bond distances, bond angles, anisotropic thermal parameters, and hydrogen atom parameters are available as supplementary material. All calculations were performed on a VAX 11/750 computer by using SDP/VAX.⁶

A pale green prismatic crystal of tetrakis(diphenyl phosphato)dimolybdenum(II,III) tetrafluoroborate having approximate dimensions of 0.40 × 0.40 × 0.80 mm was mounted in a glass capillary with its long axis roughly parallel to the φ axis of the goniometer. Cell constants and an orientation matrix for data collection were obtained from least-squares refinement, by using the setting angles of 20 reflections in the range 20° < 2θ < 24°. The triclinic cell parameters and calculated volume are as follows: $a = 10.917(8)$, $b = 11.793(4)$, $c = 12.430(4)$ Å; $\alpha = 63.45(2)$, $\beta = 70.38(4)$, $\gamma = 70.64(5)$ °; $V = 1316.8(12)$ Å³. For $Z = 1$ the calculated density is 1.61 g/cm³. As a check on crystal quality, ω scans of several intense reflections were measured; the width at half-height was 0.28° with a take-off angle of 6.0°, indicating good crystal quality. From subsequent least-squares refinement, the space group was determined to be P $\bar{1}$ (No. 2).

A total of 12 192 reflections were collected, of which 6096 were unique and not systematically absent ($R_{\text{MERGE}}(I) = 0.012$). A linear decay correction, based on three representative reflections, was applied; the correction factors on F ranged from 1.000 to 1.005 with an average value of 1.002.

Lorentz and polarization corrections were applied to the data. The linear absorption coefficient is 6.6 cm⁻¹ for Mo K α radiation. A numerical absorption correction was made to yield relative transmission coefficients ranging from 0.779 to 0.828 with an average value of 0.807. A secondary extinction correction was applied.⁷

The structure was solved by using the Patterson heavy-atom method which revealed the positions of the Mo and O atoms. The remaining atoms were located in succeeding difference Fourier syntheses. Hydrogen atoms were refined isotropically. The structure was refined by full-matrix least-squares where the function minimized was $\sum w(|F_o| - |F_c|)^2$, and the weight w is defined as 1.0 for all observed reflections.

Scattering factors were taken from Cromer and Waber.⁸ Anomalous dispersion effects were included in F_c ; the values for $\Delta f'$ and $\Delta f''$ were those of Cromer.¹⁰ Only the 4954 reflections having intensities greater than 3.0 times their standard deviation were used in the refinements. The final cycle of refinement, which included 433 variable parameters, converged (largest parameter shift was 0.90 times its esd) with $R = 0.036$ and $R_w = 0.043$. The standard deviation of an observation of unit weight was 1.061.

Instrumentation. Absorption spectra were recorded on Cary 17D or Cary 2300 spectrophotometers. Extinction coefficients were determined by using high-vacuum cells consisting of a 1-cm quartz cuvette and a 10-mL side arm. These two chambers were separated with two Kontes high-vacuum quick-release Teflon stopcocks. For measurements of molar absorptivity coefficients, weighed samples were placed in the cuvette and isolated by the Kontes valve. The appropriate high-purity solvent was transferred to the 10-mL side arm by bulb-to-bulb vacuum distillation or by syringe from a calibrated volumetric vessel, and three subsequent freeze-pump-thaw cycles were performed before mixing with the sample. Extinction coefficients were calculated from Beer-Lambert plots composed of at least seven points.

The oxidation-reduction potentials of the dimolybdenum complexes were determined by cyclic voltammetry with a Princeton Applied Research (PAR) Model 173 potentiostat, Model 175 programmer, and a Model 179 digital coulometer. The output of the digital coulometer was fed directly into a Houston Instrument Model 2000 X-Y recorder. Cyclic voltammetry measurements were performed at room temperature by using a H-cell specially designed for anaerobic, nonaqueous environments,¹¹ and a three-electrode system consisting of a Pt button electrode ($A = 0.08$ cm²), a Pt wire auxiliary electrode, and an Ag wire provided a reference potential with ferrocene used as the internal standard. Potentials were related to the SCE reference scale by using a ferrocenium-ferrocene couple of 0.307 V vs SCE.¹²

Sample irradiations for photochemical experiments were executed by using a Hanovia 1000-W Hg/Xe high-pressure lamp. The beam was collimated and passed through a 10-cm circulating water filter. Photolysis experiments were performed in two-arm evacuable cells equipped with

- (6) Frenz, B. A. In *Computing in Crystallography*; Schenk, H., Olthoff-Hazelkamp, R., van Koningsveld, H., Bassi, G. C., Eds; Delft: Delft, Holland; 1978; p 64.
- (7) Zachariasen, W. H. *Acta Crystallogr.* **1963**, *16*, 1139.
- (8) Cromer, D. T.; Waber, J. T. *International Tables for X-Ray Crystallography*; Kynoch: Birmingham, U.K., 1974; Vol. IV, Table 2.2B.
- (9) Ibers, J. A.; Hamilton, W. C. *Acta Crystallogr.* **1964**, *17*, 781.
- (10) Cromer, D. T.; Waber, J. T. *International Tables for X-Ray Crystallography*; Kynoch: Birmingham, U.K., 1974; Vol. IV, Table 2.3.1.
- (11) Mussell, R. D.; Nocera, D. G. *Inorg. Chem.* **1990**, *29*, 3711.
- (12) Gagne, R. R.; Koval, C. A.; Lisensky, G. C. *Inorg. Chem.* **1980**, *19*, 2854.

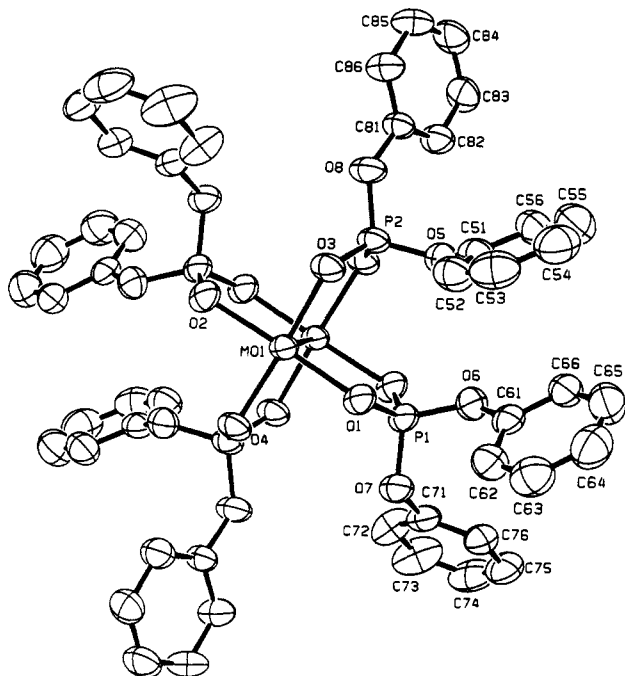


Figure 1. ORTEP view of the structure of the mixed-valence $\text{Mo}_2[\text{O}_2\text{P}(\text{OC}_6\text{H}_5)_2]_4\text{BF}_4$. Thermal ellipsoids are drawn at the 50% probability level.

Kontes quick-release teflon valves. Sample temperatures were thermostated at 15.0 ± 0.5 °C in all photoreactions. Photolyses were accomplished by using Schott color glass high-energy cutoff filters to eliminate the unwanted higher energy light. For quantum yield measurements, the 546-nm excitation wavelength was isolated by using an interference filter purchased from Oriol Corporation with a half-width of less than 10 nm at the mercury line. Quantum yields were determined on 7 M solutions of the dichlorocarbon in benzene by monitoring the disappearance of $\text{Mo}_2[\text{O}_2\text{P}(\text{OC}_6\text{H}_5)_2]_4$ at 515 nm and appearance of $\text{Mo}_2[\text{O}_2\text{P}(\text{OC}_6\text{H}_5)_2]_4^+$ at 1494 nm ($\epsilon = 362 \text{ M}^{-1} \text{ cm}^{-1}$). The absolute quantum yield for photoreduction of 1,2-dichloroethane was measured by using a ferrioxalate actinometer; the quantum yields for reaction of all other halocarbon solutions were measured relative to 1,2-dichloroethane.

Volatile organic photoproducts were identified by GC/MS, the instrument for which consisted of a Hewlett-Packard 5890J GC modified for coupling to a JEOL JMS-AX505H double-focusing MS. Separations were achieved on a poraplot U fused silica capillary column from Chrompack (25-m length, 0.32-mm i.d., 10- μm film thickness). The m/z scans ranged from 15 to 400, and the GC column temperature was programmed from 30 to 200 °C at 10 °C/min. Organic products that were liquids were analyzed on a HP 5890 GC/TRIO-1 MS instrument up to masses of 1000. The column is an SE-54 support-coated open tubular capillary column from Alltech with 30-m length (0.32-mm i.d., 0.25- μm film thickness). The mass spectrometer ion source was maintained at 200 °C, and the GC column temperature was programmed from 35 to 200 °C at 5 °C/min. For both instruments, the helium carrier gas was set at a flow rate of 1 mL/min. The organic photoproducts were separated from photoreacted solutions by vacuum distillation, and 1 μL of liquid sample was employed by splitless injection.

Results and Discussion

Structural Chemistry. Our X-ray crystal determination of the $\text{Mo}_2[\text{O}_2\text{P}(\text{OC}_6\text{H}_5)_2]_4\cdot 2\text{THF}$ yielded results similar to MT, but the crystal and space groups are different. Thus the results of the crystal structure determination of $\text{Mo}^{\text{II}}\text{Mo}^{\text{II}}$ tetrakis(diphenyl phosphate) are included as supplementary material and only the crystal structure of the mixed-valence compound $\text{Mo}_2[\text{O}_2\text{P}(\text{OC}_6\text{H}_5)_2]_4\text{BF}_4$ is emphasized here. Figure 1 shows the molecular structure and atom-numbering scheme for the mixed-valence complex, and Table 3 lists selected bond distances and bond angles. For convenience of comparison, the same numbering atom scheme established by MT for the the quadruple bond complex is used in Figure 1.

Table 3. Selected Bond Lengths (Å) and Angles (deg) for $\text{Mo}_2[\text{O}_2\text{P}(\text{OC}_6\text{H}_5)_2]_4\text{BF}_4$

Bond Lengths			
Mo(1)–Mo(1)	2.190	P(1)–O(6)	1.557(3)
Mo(1)–O(1)	2.081(2)	P(1)–O(7)	1.571(3)
Mo(1)–O(2)	2.069(2)	P(2)–O(3)	1.512(4)
Mo(1)–O(3)	2.074(2)	P(2)–O(4)	1.512
Mo(1)–O(4)	2.077(3)	P(2)–O(5)	1.562(3)
P(1)–O(1)	1.512(3)	P(2)–O(8)	1.564(2)
P(1)–O(2)	1.510		
Bond Angles			
Mo(1)–Mo(1)–O(1)	94.5	O(2)–Mo(1)–O(3)	88.6(1)
Mo(1)–Mo(1)–O(2)	94.9	O(2)–Mo(1)–O(4)	90.0(1)
Mo(1)–Mo(1)–O(3)	94.7	O(3)–Mo(1)–O(4)	170.9(1)
Mo(1)–Mo(1)–O(4)	94.4	Mo(1)–O(1)–P(1)	117.8(1)
O(1)–Mo(1)–O(2)	170.5(1)	Mo(1)–O(2)–P(1)	118.1
O(1)–Mo(1)–O(3)	89.79(9)	Mo(1)–O(3)–P(2)	117.0(1)
O(1)–Mo(1)–O(4)	90.1(1)	Mo(1)–O(4)–P(2)	117.2

Even though the molecular structures of the $\text{Mo}^{\text{II}}\text{Mo}^{\text{II}}$ and $\text{Mo}^{\text{II}}\text{Mo}^{\text{III}}$ compounds appear similar, closer examination reveals some significant differences between the two molecules. The most noticeable difference is the Mo–Mo bond distance which increases from 2.141 Å in $\text{Mo}_2[\text{O}_2\text{P}(\text{OC}_6\text{H}_5)_2]_4\cdot 2\text{THF}$ to 2.191 Å in $\text{Mo}_2[\text{O}_2\text{P}(\text{OC}_6\text{H}_5)_2]_4\text{BF}_4$ despite the weak axial coordination of THF molecules to the quadruply bonded metal–metal core. This increase of 0.05 Å resulting from the oxidation of the dimer by one electron is comparable to that observed for the multiply bonded Mo_2 sulfates, which also exhibit a lengthening of the Mo–Mo bond by 0.05 Å upon one-electron oxidation of the metal–metal core (2.111 and 2.164 Å for quadruple bond and mixed-valence complexes, respectively).¹³ The increase is expected and is attributed to the reduced δ bond order of the mixed-valence complex.¹⁴ Additionally, an increase in formal charge on each metal (from +2 to +2.5) causes a constriction of the valence orbitals of the metal atoms and corresponding decreased orbital overlap.

Because of the longer metal–metal bond distance in the mixed-valence species, there is less steric strain associated with the bridging phosphate ligands. The Mo_2O_2 segments of the five-membered $\text{Mo}_2(\text{O}_2\text{P})$ rings are planar (maximum deviation from planarity ± 0.007 Å) and orthogonal to each other (dihedral angle of 90.3°). As is the case for the quadruple bond analog, the phosphorus atoms deviate significantly from the Mo_2O_2 planes, and the five-membered rings are thereby puckered. The slightly smaller dihedral angles between the $\text{Mo}_2\text{O}_2\cdots\text{O}_2\text{P}$ planes of the mixed-valence structure (i.e. planes hinged through the oxygen atoms are defined by dihedral angles of 8.8/18.9° and 14.5/18.9° for $\text{Mo}_2[\text{O}_2\text{P}(\text{OC}_6\text{H}_5)_2]_4\text{BF}_4$ and $\text{Mo}_2[\text{O}_2\text{P}(\text{OC}_6\text{H}_5)_2]_4\cdot 2\text{THF}$, respectively) most probably reflect relaxed steric constraints imposed by the metal–metal bond distance. Moreover whereas there is no significant difference between the $\text{Mo}^{\text{II}}\text{Mo}^{\text{II}}$ and $\text{Mo}^{\text{II}}\text{Mo}^{\text{III}}$ complexes for oxygen bonded to phosphorus (average O–P distances of $\text{O}_2\text{P}(\text{OC}_6\text{H}_5)_2^-$ chelated to $\text{Mo}^{\text{II}}\text{Mo}^{\text{II}}$ and $\text{Mo}^{\text{II}}\text{Mo}^{\text{III}}$ cores are 1.500(7) and 1.512(3) Å, respectively), the Mo–O bond lengths of the $\text{Mo}^{\text{II}}\text{Mo}^{\text{III}}$ compound are 0.05–0.07 Å shorter than those of the $\text{Mo}^{\text{II}}\text{Mo}^{\text{II}}$ compound. This observation, which is also observed in the dimolybdenum sulfate system, is entirely consistent with the increased positive charge of the mixed-valence core.

Oxidation–Reduction Chemistry. The cyclic voltammogram of $\text{Mo}_2[\text{O}_2\text{P}(\text{OC}_6\text{H}_5)_2]_4$ in CH_2Cl_2 is shown in Figure 2a. In contrast to the studies of MT, two reversible oxidation processes are observed upon anodically scanning solutions containing the quadruple bond complex. Reversible electrochemical behavior for these two waves is indicated by linear plots of the cathodic and anodic currents vs $v^{1/2}$ (scan rate, 20–200 mV s^{-1}), and values

(13) Cotton, F. A.; Frenz, B. A.; Pedersen, E.; Webb, T. R. *Inorg. Chem.* **1975**, *14*, 391.

(14) Cotton, F. A.; Walton, R. A. *Multiple Bonds Between Metal Atoms*, 2nd ed.; Oxford: New York, 1993; Chapter 10, p 632.

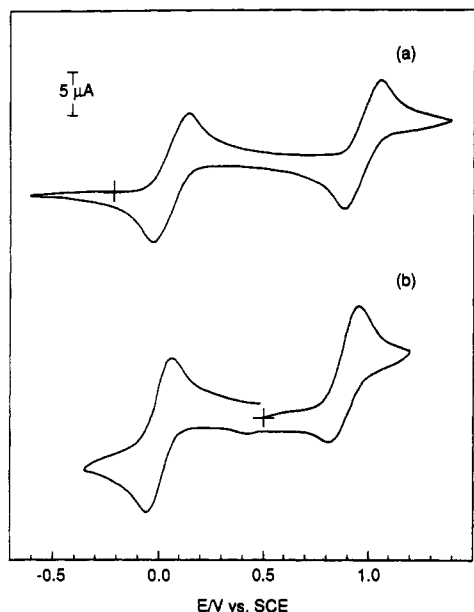


Figure 2. Cyclic voltammograms of (a) $\text{Mo}_2[\text{O}_2\text{P}(\text{OC}_6\text{H}_5)_2]_4$ and (b) $\text{Mo}_2[\text{O}_2\text{P}(\text{OC}_6\text{H}_5)_2]_4\text{BF}_4$ in CH_2Cl_2 solution at 23°C . NBu_4PF_6 was used as the supporting electrolyte, and the scan rate was 20 mV s^{-1} for (a) and 100 mV s^{-1} for (b).

Table 4. Formal Reduction Potentials of the $\text{Mo}^{\text{II}}\text{Mo}^{\text{III}}/\text{Mo}^{\text{II}}\text{Mo}^{\text{II}}$ and $\text{Mo}^{\text{III}}\text{Mo}^{\text{III}}/\text{Mo}^{\text{II}}\text{Mo}^{\text{III}}$ Couples of Dimolybdenum Tetrakis(sulfate), -(phosphate), and -(diphenyl phosphate) Complexes

complex	$E_{1/2}/\text{V vs SCE}$	
	$\text{Mo}^{\text{II}}\text{Mo}^{\text{III}}/\text{Mo}^{\text{II}}\text{Mo}^{\text{II}}$	$\text{Mo}^{\text{III}}\text{Mo}^{\text{III}}/\text{Mo}^{\text{II}}\text{Mo}^{\text{III}}$
sulfate	+0.25 ^a	
phosphate	-0.67 ^b	-0.24 ^b
diphenyl phosphate	+0.06 ^c	+1.00 ^c

^a Reference 13. ^b Reference 2. ^c This work.

of 0.99 ± 0.02 for ratios of the anodic and cathodic peak currents. Figure 2b illustrates the cyclic voltammogram of the mixed-valence species $\text{Mo}_2[\text{O}_2\text{P}(\text{OC}_6\text{H}_5)_2]_4\text{BF}_4$ in CH_2Cl_2 . Anodic and cathodic scans of the electrode potential from the resting potential of the solution yield a cyclic voltammogram identical to the Mo^{II} - Mo^{II} complex with $E_{1/2}$ values of -0.24 and $+0.69\text{ V}$ vs the ferrocene internal standard (and thus $+0.067$ and 0.997 V vs SCE). These results clearly establish that the waves at $+0.067$ and 0.997 V vs SCE correspond to the $\text{Mo}_2[\text{O}_2\text{P}(\text{OC}_6\text{H}_5)_2]_4^{0/+}$ and $\text{Mo}_2[\text{O}_2\text{P}(\text{OC}_6\text{H}_5)_2]_4^{+/2+}$ couples, respectively.

A comparison of these data with previously reported oxidation-reduction properties of multiply bonded " Mo_2O_8 " complexes offers the opportunity to assess the perturbation of oxo ligating spheres on the redox chemistry of dimolybdenum cores. Table 4 collects the reduction potentials for $\text{Mo}_2(\text{SO}_4)_4^{4-}$,¹³ $\text{Mo}_2(\text{HPO}_4)_4^{4-}$,² and $\text{Mo}_2[\text{O}_2\text{P}(\text{OC}_6\text{H}_5)_2]_4$. The $\text{Mo}^{\text{II}}\text{Mo}^{\text{III}}/\text{Mo}^{\text{II}}\text{Mo}^{\text{II}}$ reduction potentials of the sulfate and diphenyl phosphate are similar and significantly positive to that for the phosphate compound. The structural and electronic properties of HPO_4^{2-} , SO_4^{2-} and $\text{O}_2\text{P}(\text{OR})_2^-$ are comparable, and it is difficult on this basis to account for the $\sim 1.0\text{-V}$ shift to negative potentials for the $\text{Mo}_2(\text{HPO}_4)_4^{4-}$ couples. However the HPO_4^{2-} is distinguished from $\text{O}_2\text{P}(\text{OR})_2^-$ and SO_4^{2-} by its chemical properties. Proton association with the sulfate and diphenyl phosphate is unlikely, whereas an equilibrium with protons of the phosphate ligand can be established in aqueous solution. To this end, the reduction potentials of the diphenyl phosphate complex lend further support to the contention² that proton equilibria involving ligands coordinating the dimolybdenum core can have a pronounced effect on its redox chemistry in solution.

Finally, the difficulty with obtaining the triply bonded dimolybdenum sulfate and diphenyl phosphate systems can be rationalized on the basis of the oxidation-reduction chemistry.

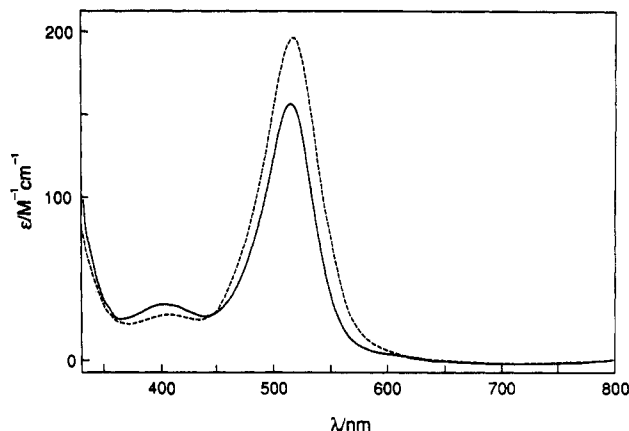


Figure 3. Electronic absorption spectra of (a) $\text{Mo}_2[\text{O}_2\text{P}(\text{OC}_6\text{H}_5)_2]_4$ (—) in CH_2Cl_2 solution and (b) $\text{Mo}_2(\text{HPO}_4)_4^{4-}$ (---) in $2\text{ M H}_3\text{PO}_4$ at 25°C .

The $\text{Mo}^{\text{III}}\text{Mo}^{\text{III}}/\text{Mo}^{\text{II}}\text{Mo}^{\text{III}}$ couple for the sulfato complex has yet to be determined. Inasmuch as the SO_4^{2-} and $\text{O}_2\text{P}(\text{OR})_2^-$ ligands are not affected by proton equilibria, we believe that the separation between the $\text{Mo}^{\text{II}}\text{Mo}^{\text{III}}/\text{Mo}^{\text{II}}\text{Mo}^{\text{II}}$ and $\text{Mo}^{\text{III}}\text{Mo}^{\text{III}}/\text{Mo}^{\text{II}}\text{Mo}^{\text{III}}$ couples should be similar for sulfato and diphenyl phosphato compounds. On this basis, we predict the latter couple of the sulfato complex to lie at $\sim 1.20\text{ V}$ vs SCE. Consequently, the inability to generate the triply bonded sulfate complex is not due to the intrinsic instability of this species, but rather because the reduction potential for the generation of the triply bonded complex lies positive of the potential for water oxidation. Similarly, attempts to prepare the triply bonded dimolybdenum diphenyl phosphate are also frustrated by the very positive $\text{Mo}^{\text{III}}\text{Mo}^{\text{III}}/\text{Mo}^{\text{II}}\text{Mo}^{\text{III}}$ couple. Although oxidation of the quadruple bond complex by NOBF_4 proceeds smoothly to $\text{Mo}_2[\text{O}_2\text{P}(\text{OC}_6\text{H}_5)_2]_4^{4+}$, oxidation to $\text{Mo}_2[\text{O}_2\text{P}(\text{OC}_6\text{H}_5)_2]_4^{2+}$ with NOBF_4 cannot be achieved because the NO^+/NO couple (estimated to be ~ 0.85 to 1.0 V vs SCE in nonaqueous solution¹⁵) is insufficient to bring about subsequent oxidation of the mixed-valence species. Even stronger one-electron oxidants, such as tris(4-bromophenyl)-ammonium hexachloroantimonate ($E_{1/2} = 1.04\text{ V}$ vs SCE) or dichloroiodobenzene (estimated $0.9\text{--}1.2\text{ V}$ vs SCE) yield only the mixed-valence product. This may result from kinetic barriers to generating the dication, which cannot be overcome by carrying out the reaction at elevated temperatures owing to decomposition of the mixed-valence complex upon heating. Alternatively, electrochemical methods may offer the dication species. Bulk electrolysis of solutions at potentials as high as 1.7 V vs SCE led to the disappearance of the near-infrared absorption of the mixed-valence dimer and the appearance of weak absorptions in the visible. Although the species in solution failed to crystallize, the spectral changes accompanying bulk electrolysis are consistent with the formation of the triply bonded dimer, and we suspect that the electrochemical preparation of this triply bonded species is plausible.

Spectroscopic Characterization. Figure 3 illustrates the electronic absorption spectrum of $\text{Mo}_2[\text{O}_2\text{P}(\text{OC}_6\text{H}_5)_2]_4$ in CH_2Cl_2 solution. Comparison to the absorption profile of $\text{Mo}_2(\text{HPO}_4)_4^{4-}$, which is also reproduced in Figure 3, reveals that substitution of HPO_4^{4-} by diphenyl phosphate does little to perturb the electronic structure of the quadruple bonded metal-metal system. The lowest energy absorption band ($\lambda_{\text{max}} = 515\text{ nm}$, $\epsilon = 156\text{ M}^{-1}\text{ cm}^{-1}$) is comparable in energy and intensity to the $\delta^2 \rightarrow \delta\delta^*$ transition of $\text{Mo}_2(\text{HPO}_4)_4^{4-}$ and is similarly flanked to higher energy by a band at 404 nm ($\epsilon = 38\text{ M}^{-1}\text{ cm}^{-1}$), which has tentatively been assigned to the $\pi \rightarrow \delta^*$ transition.² Parallel trends are also observed between the electronic absorption spectra of the mixed-valence complexes of the dimolybdenum phosphate

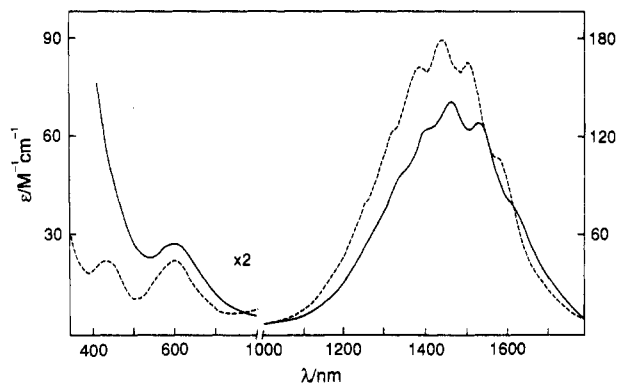
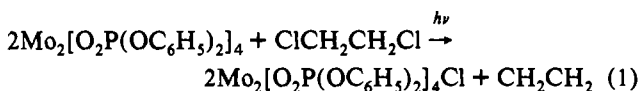


Figure 4. Electronic absorption spectrum of the mixed-valence (a) $\text{Mo}_2[\text{O}_2\text{P}(\text{OC}_6\text{H}_5)_2]_4\text{BF}_4$ (—) in CH_2Cl_2 solution and (b) $\text{Mo}_2(\text{HPO}_4)_4^{3-}$ (---) in 2 M H_3PO_4 at 25 °C.

and diphenyl phosphate systems (Figure 4). As reported by MT, $\text{Mo}_2[\text{O}_2\text{P}(\text{OC}_6\text{H}_5)_2]_4\text{BF}_4$ exhibits a prominent absorption band in the near-infrared ($\lambda_{\text{max}} = 1469 \text{ nm}$, $\epsilon = 142 \text{ M}^{-1} \text{ cm}^{-1}$) that is consistent with an assignment to the $\delta \rightarrow \delta^*$ ($2\text{B}_{1u} \leftarrow 2\text{B}_{2g}$) transition.^{3a,16} The band features vibrational structure for solution spectra at room temperature, which becomes more highly resolved at low temperatures. The 308-cm^{-1} energy spacing is consistent with a progression in the symmetric metal–metal stretching vibration. As with dimolybdenum phosphate and sulfate, the large red-shift of the $\delta \rightarrow \delta^*$ transition in mixed-valence $\text{Mo}^{\text{II}}\text{-Mo}^{\text{III}}$ complex is explained by the absence of two electron spin pairing terms of a $\sigma^2\pi^4\delta^1$ ground-state configuration.¹⁷ The 600-nm band ($\epsilon = 27 \text{ M}^{-1} \text{ cm}^{-1}$) in $\text{Mo}_2[\text{O}_2\text{P}(\text{OC}_6\text{H}_5)_2]_4\text{BF}_4$ is directly analogous to the lower energy absorption in $\text{Mo}^{\text{II}}\text{Mo}^{\text{III}}$ sulfato and phosphato complexes and by analogy is assigned to the $\pi \rightarrow \delta$ transition. Higher energy absorptions in the visible spectral region are apparently obscured by the tail of strong ultraviolet absorptions arising from intraligand $\pi \rightarrow \pi^*$ transitions of the aromatic rings.

In spite of these spectroscopic similarities between $\text{Mo}_2[\text{O}_2\text{P}(\text{OC}_6\text{H}_5)_2]_4$ and $\text{Mo}_2(\text{HPO}_4)_4^{4-}$, the former is distinguished by a weak luminescence ($\phi_{\text{em}} = 5 \times 10^{-4}$) in nonaqueous solution and a $^1(\delta\delta^*)$ excited-state lifetime of 68 ns.⁴ This appreciable lifetime, in conjunction with the energy of the $^1(\delta\delta^*)$ excited state ($E_{1/2}(\text{Mo}_2[\text{O}_2\text{P}(\text{OC}_6\text{H}_5)_2]_4^{+/}) = 2.24 \text{ eV}$),¹⁸ engenders photochemical reactivity of the quadruple bond complex with organic substrates.

Photochemistry. Whereas 1,2-dichloroethane solutions of $\text{Mo}_2[\text{O}_2\text{P}(\text{OC}_6\text{H}_5)_2]_4$ are indefinitely stable in the absence of light, we have observed prompt reaction of halocarbon solutions of $\text{Mo}_2[\text{O}_2\text{P}(\text{OC}_6\text{H}_5)_2]_4$ upon visible irradiation with wavelengths of light energetically coincident with the $\delta\delta^*$ transition. The two-electron conversion of 1,2-dichloroethane to ethylene occurs by the following reaction:⁴



We have explored the DCE photoreaction further by studying the solvent dependence of the quantum yield. As shown in Table 5, the quantum yield for photoreaction decreases dramatically with the increasing ability of solvent to ligate the metal core. The reduction of alkyl halides by transition metal donors can occur

Table 5. Quantum Yield Data for the Photoreaction between $\text{Mo}_2[\text{O}_2\text{P}(\text{OC}_6\text{H}_5)_2]_4$ and 1,2-Dichlorocarbons in Various Nonaqueous Solvents

1,2-dichlorocarbon	solvent	ϕ_p^a
1,2-dichloroethane	C_6H_6	0.029
1,2-dichloroethane	THF	0.014
1,2-dichloroethane	CH_3CN	0.0012
1,2-dichlorocyclohexane	C_6H_6	0.040
1,2-dichloroethylene	C_6H_6	5.5×10^{-6}
<i>o</i> -dichlorobenzene	C_6H_6	1.4×10^{-4}

^a Quantum yield for the photoreaction ($\lambda_{\text{exc}} = 546 \text{ nm}$) of $\text{Mo}_2[\text{O}_2\text{P}(\text{OC}_6\text{H}_5)_2]_4$ with dichlorocarbon as determined by using a ferrioxalate actinometer. The concentration of chlorocarbon is 7 M.

by outer-sphere¹⁹ or inner-sphere electron-transfer pathways,^{19d,20} with the latter being especially important for transition metal reductants featuring open coordination sites. In view of the vacant axial coordination sites of the metal–metal core, an inner-sphere reaction pathway is likely to play a significant role in the photoreduction of alkyl halides by electronically excited $\text{Mo}^{\text{II}}\text{-Mo}^{\text{III}}$ diphenyl phosphate complex. In support of this contention is the crystal structure of $\text{Mo}_2[\text{O}_2\text{P}(\text{OC}_6\text{H}_5)_2]_4 \cdot 2\text{THF}$, which shows an inaccessible metal–metal core upon axial coordination of solvent. Not surprisingly, Table 5 reveals that the photoreduction of DCE by $\text{Mo}_2[\text{O}_2\text{P}(\text{OC}_6\text{H}_5)_2]_4$ is significantly diminished in THF. These data suggest that the photoreaction is confined predominantly to the axial coordination site of the metal–metal core.

The $\text{Mo}_2[\text{O}_2\text{P}(\text{OC}_6\text{H}_5)_2]_4$ dimer also reacts with other 1,2-dihalocarbons including 1,2-dichlorocyclohexane (DCC), *cis*-1,2-dichloroethylene (DCEE), and *o*-dichlorobenzene (DCB). Similar to DCE photochemistry, photoreduction of these halocarbons is signified by the disappearance of the $\delta \rightarrow \delta^*$ transition of $\text{Mo}_2[\text{O}_2\text{P}(\text{OC}_6\text{H}_5)_2]_4$ at 515 nm and the concomitant growth of this same absorption for the mixed-valence complex $\text{Mo}_2[\text{O}_2\text{P}(\text{OC}_6\text{H}_5)_2]_4\text{Cl}$ at 1494 nm. This red shift in the $\delta \rightarrow \delta^*$ absorption band with respect to the BF_4^- salt is attributed to the presence of chloride ion in photolyzed solutions.⁴ With respect to the organic photoproducts, the DCC and DCE photochemistry is analogous inasmuch as GC/MS shows the exclusive production of the unsaturated olefin (cyclohexene, $[\text{M}]^+ = m/z 82$, $[\text{M} - \text{CH}_3]^+ = m/z 67$, $[\text{M} - \text{C}_2\text{H}_4]^+ = m/z 54$, $[\text{M} - \text{C}_3\text{H}_5]^+ = m/z 41$, and $[\text{M} - \text{C}_3\text{H}_7]^+ = m/z 39$).²¹ However, when the substrate is an unsaturated dichlorocarbon, the organic photoproduct is not the olefin hydrocarbon. Consider the photochemistry of DCB. Elimination of chlorine from DCB would result in benzyne, which is efficiently trapped by furan to yield α -naphthol. Yet when $\text{Mo}_2[\text{O}_2\text{P}(\text{OC}_6\text{H}_5)_2]_4$ is irradiated in the presence of DCB and furan, α -naphthol is not detected; GC/MS reveals chlorobenzene as the principal photoproduct (Figure 5a). In addition to chlorobenzene, a high-boiling fraction is also isolated from the photoreaction mixture; its GC/MS (Figure 5b) shows it to be primarily trichlorobiphenyl. The photoproduction of monochlorinated product is consistent with chlorine abstraction by the photoexcited quadruple bond species, but subsequent elimination of chlorine from the incipient chlorobenzyl radical does not occur. The appearance of polychlorinated biphenyls is consistent with initial chlorine atom abstraction owing to the known reaction of

(16) Fanwick, P. E.; Martin, D. S.; Webb, T. R.; Robbins, G. A.; Newman, R. A. *Inorg. Chem.* **1978**, *17*, 2723.

(17) Hopkins, M. D.; Gray, H. B.; Miskowski, V. M. *Polyhedron* **1987**, *6*, 705.

(18) The reduction potential of an excited state was calculated from $E_{1/2}(\text{Mo}_2[\text{O}_2\text{P}(\text{OC}_6\text{H}_5)_2]_4^{+/}) = E_{1/2}(\text{Mo}_2[\text{O}_2\text{P}(\text{OC}_6\text{H}_5)_2]_4^{0/}) - E_{0-0}(\text{Mo}_2[\text{O}_2\text{P}(\text{OC}_6\text{H}_5)_2]_4^{+/})$, where the electronic origin, E_{0-0} , was estimated from the emission spectrum to be 2.31 eV.

(19) (a) Bakac, A.; Espenson, J. H. *J. Am. Chem. Soc.* **1986**, *108*, 713. (b) Andrieux, C. P.; Gallardo, I.; Savéant, J.-M.; Su, K.-B. *J. Am. Chem. Soc.* **1986**, *108*, 638. (c) Lexa, D.; Savéant, J.-M.; Schafer, H. J.; Su, K.-B.; Vering, B.; Wang, D. L. *J. Am. Chem. Soc.* **1990**, *112*, 6162. (d) Andrieux, C. P.; Le Gorande, A.; Savéant, J.-M. *J. Am. Chem. Soc.* **1992**, *114*, 6892. (e) Savéant, J.-M. *J. Am. Chem. Soc.* **1992**, *114*, 10595.

(20) (a) Savéant, J.-M. *J. Am. Chem. Soc.* **1987**, *109*, 6788. (b) Lexa, D.; Savéant, J.-M.; Su, K.-B.; Wang, D. L. *J. Am. Chem. Soc.* **1988**, *110*, 7617. (c) Savéant, J.-M. *Adv. Phys. Org. Chem.* **1990**, *26*, 1.

(21) Heller, S. R.; Milne, G. W. A. *EPA/NIH Mass Spectral Data Base*; U. S. Department of Commerce/National Bureau of Standards: Washington, DC, 1978; Vol. I.

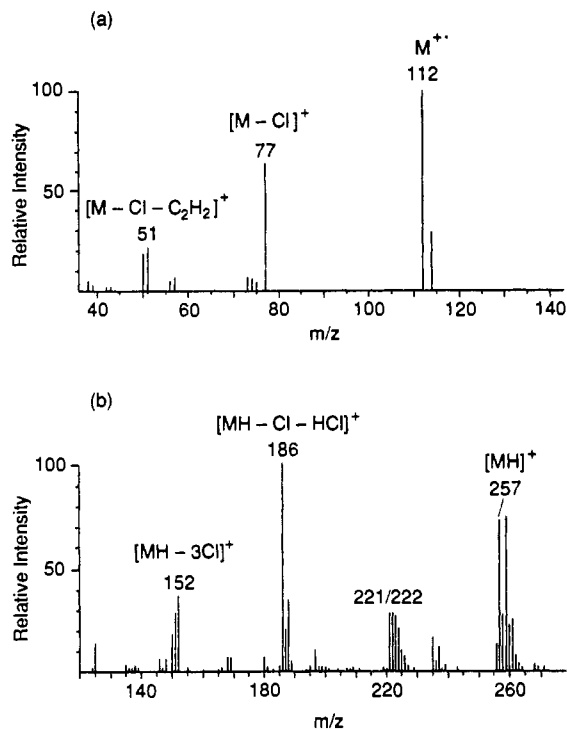
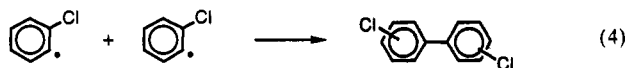
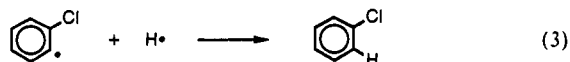


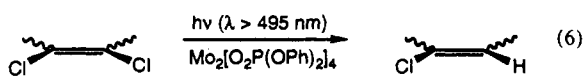
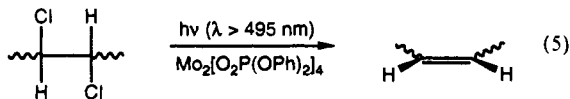
Figure 5. Mass spectra of the organic products resulting from the photoreaction of *o*-dichlorobenzene with $\text{Mo}_2[\text{O}_2\text{P}(\text{OC}_6\text{H}_5)_2]_4$ with (a) chlorobenzene obtained as the primary product and (b) trichlorobiphenyl obtained as a secondary product detected as $[\text{M} + \text{H}]^+$ self-Cl product at m/z 257.

the chlorobenzyl radical with DCB:²²



The photoreactivity $\text{Mo}_2[\text{O}_2\text{P}(\text{OC}_6\text{H}_5)_2]_4$ with DCEE is similar to that of DCB with the monohalogenated olefin observed as the photoproduct (chloroethylene, $[\text{M}]^+ = m/z$ 62, $[\text{M} - \text{Cl}]^+ = m/z$ 27).

The general result to emerge from our product distribution studies is summarized by eqs 5 and 6. Initial chlorine abstraction



by photoexcited $\text{Mo}_2[\text{O}_2\text{P}(\text{OC}_6\text{H}_5)_2]_4$ leads to the olefin hydrocarbon when the substrate is a saturated dichlorocarbon whereas unsaturated dihalocarbons react to produce monohalogenated olefin. In both cases, the inorganic photoproduct is the mixed-valence $\text{Mo}^{\text{II}}\text{Mo}^{\text{III}}$ species. The difficulty with driving the photochemistry of the diphenyl phosphate systems to the two-electron oxidized $\text{Mo}^{\text{III}}\text{Mo}^{\text{III}}$ core of the triply bonded complex

arises from the inaccessibility of the $\text{Mo}^{\text{III}}\text{Mo}^{\text{III}}/\text{Mo}^{\text{II}}\text{Mo}^{\text{III}}$ couple. This points to a difference between the photochemistry of the phosphato and diphenyl phosphato systems. For the former, the $\text{Mo}^{\text{III}}\text{Mo}^{\text{III}}$ complex is obtained as the photoproduct because of the -1.0-V shift of the $\text{Mo}^{\text{III}}\text{Mo}^{\text{III}}/\text{Mo}^{\text{II}}\text{Mo}^{\text{III}}$ couple to less positive potentials.

Table 5 shows the quantum yields for the photoreaction for the selected substrates with $\text{Mo}_2[\text{O}_2\text{P}(\text{OC}_6\text{H}_5)_2]_4$. The mechanism for eq 5 is consistent with chlorine abstraction by the electronically excited $\text{Mo}_2[\text{O}_2\text{P}(\text{OC}_6\text{H}_5)_2]_4$ complex to produce $\text{C}^\bullet\text{HCHCl}$ and the mixed-valence $\text{Mo}^{\text{II}}\text{Mo}^{\text{III}}$ complex, $\text{Mo}_2[\text{O}_2\text{P}(\text{OC}_6\text{H}_5)_2]_4\text{-Cl}$. Subsequent reaction of the radical with another 1 equiv of the $\text{Mo}^{\text{II}}\text{Mo}^{\text{II}}$ reactant, which is in excess, directly yields the observed photoproducts. The photogenerated chloroalkane radical is a very reactive species, and its thermal reaction with quadruple bond species to yield ethylene or cyclohexene is thermodynamically favorable.⁴ For eq 6, we have yet to define the intimate mechanistic details of the reaction. Aromatic and vinylic dibromides have been shown to react with low-valent metalloporphyrins by X^+ atom departure to produce a carbanion.^{19c} This E2 mechanism presumably is preferred owing to the presence of the π^* orbital. However, in this case, the direct production of the carbanion may be precluded by the high potential for production of $\text{Mo}^{\text{III}}\text{Mo}^{\text{III}}$, which is necessary for direct X^+ transfer. Alternatively, a carbanion may be produced by electron transfer of chloroalkene radical $\text{C}^\bullet=\text{CCl}$ with the $\text{Mo}^{\text{II}}\text{Mo}^{\text{II}}$ starting reagent. In either case, the monohalogenated product is obtained by protonation of the carbanion. Or does the radical simply abstract a hydrogen atom to produce the monohalogenated olefin? We do know that the radical can go on to react with olefin starting material to yield polyaromatic halocarbons. But this latter reaction occurs in small yields (<3%) and appears to be an insignificant side reaction and, therefore, may not be indicative of the primary reaction pathway.

It should be noted that the photoreduction of dichlorocarbons by $\text{Mo}_2[\text{O}_2\text{P}(\text{OC}_6\text{H}_5)_2]_4$ is consistent with the chemistry observed in the electroreduction of 1,2-dihaloalkanes and 1,2-dihaloalkenes. The early studies of von Stackelberg and Stracke established that the electroreduction of 1,2-dihalides afforded olefinic hydrocarbons.²³ The considerable body of data since these early studies corroborate this general reaction chemistry.²⁴ For 1,2-dihaloalkenes, reductions may occur via a carbanion, which is then trapped by a proton to produce the monosubstituted haloalkenes.²⁵ *cis*-2,3-Dichloroacrylonitrile is electrochemically reduced by two electrons to yield 2-chloroacrylonitrile.²⁶ In this case, reduction is believed to lead to the carbanion.

Acknowledgment. D.G.N. is an Alfred P. Sloan Fellow. We thank Dr. Rui Huang for assistance in obtaining GC/MS spectra. Financial support of this work by the National Science Foundation Grant CHE-9100532 is gratefully acknowledged. Mass spectral data were obtained at the Michigan State University Mass Spectrometry Facility, which is supported, in part, by a grant (DRR-00480) from the Biotechnology Resources Branch, Division of Research Resources, National Institutes of Health.

Supplementary Material Available: For $\text{Mo}_2[\text{O}_2\text{P}(\text{OC}_6\text{H}_5)_2]_4\text{BF}_4$ complete tables of crystal data, atomic coordinates, bond distances and angles, and anisotropic temperature factors and a stereoview of the unit cell and for $\text{Mo}_2[\text{O}_2\text{P}(\text{OC}_6\text{H}_5)_2]_4\cdot 2\text{THF}$ complete tables of crystal data, atomic coordinates, bond distances and angles, and anisotropic temperature factors and an ORTEP diagram with numbering and a stereoview of the unit cell (38 pages). Ordering information is given on any current masthead page.

(22) Uyeta, M.; Tave, S.; Chikasawa, K.; Mazaki, M. *Nature* 1976, 264, 583.

(23) von Stackelberg, M.; Stracke, W. *Z. Electrochem.* 1949, 53, 118.
 (24) Casanova, J.; Ebersson, L. In *The Chemistry of the Carbon-halogen Bond*; Patai, S., Ed.; Wiley-Interscience: New York, 1973; Chapter 15.
 (25) (a) Bunnett, J. F. *Acc. Chem. Res.* 1992, 25, 2. (b) Bolton, R.; Moore, C.; Sandall, J. P. B. *J. Chem. Soc., Perkin Trans.* 1982, 2, 1593. (c) Bard, R. R.; Bunnett, J. F.; Traber, R. P. *J. Org. Chem.* 1979, 44, 4918.
 (26) Jura, W. H.; Gaul, R. J. *J. Am. Chem. Soc.* 1958, 80, 5402.